Electronic Supplementary Material (ESI) for Dalton Transactions.

Sulfur-doped carbonized bacterial cellulose as flexible binder-free 3D anode for improve sodium ion storage

Xiangmei Wang[a], Xin Xiao [a, b, *], Chuntao Chen [a], Bianjing Sun [a], Xinyu Chen [a], Jiacheng Hu [a], Lei Zhang [a, *], Dongping Sun[a, *]

a. Institute of Chemicobiology and Functional Materials, School of Chemistry and Chemical Engineering, Nanjing University of Science and Technology, 200 Xiao Ling Wei Street, Nanjing 210094, China.

b. Jiangsu Key Laboratory of Marine Bioresources and Environment, Jiangsu Ocean University, Lianyungang 222005, China.

E-mail: xiaoxin@njust.edu.cn; leizhang@njust.edu.cn; sundpe301@163.com

---

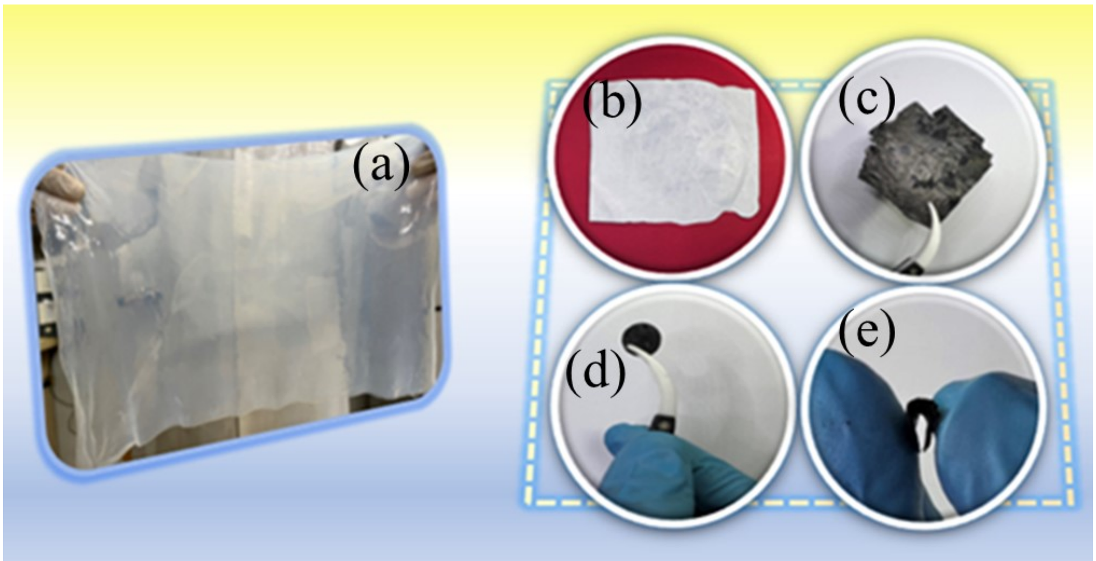

Fig. S1. The physical image of the (a)fermentation-purified BC, (b) BC aerogel and (c-e) S-CBC.

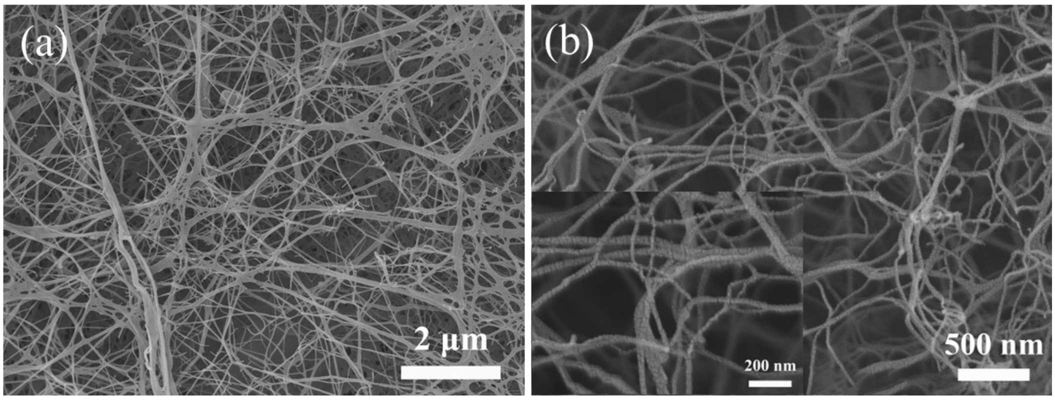

Fig. S2. (a) SEM image of BC, and (b) SEM images of CBC.

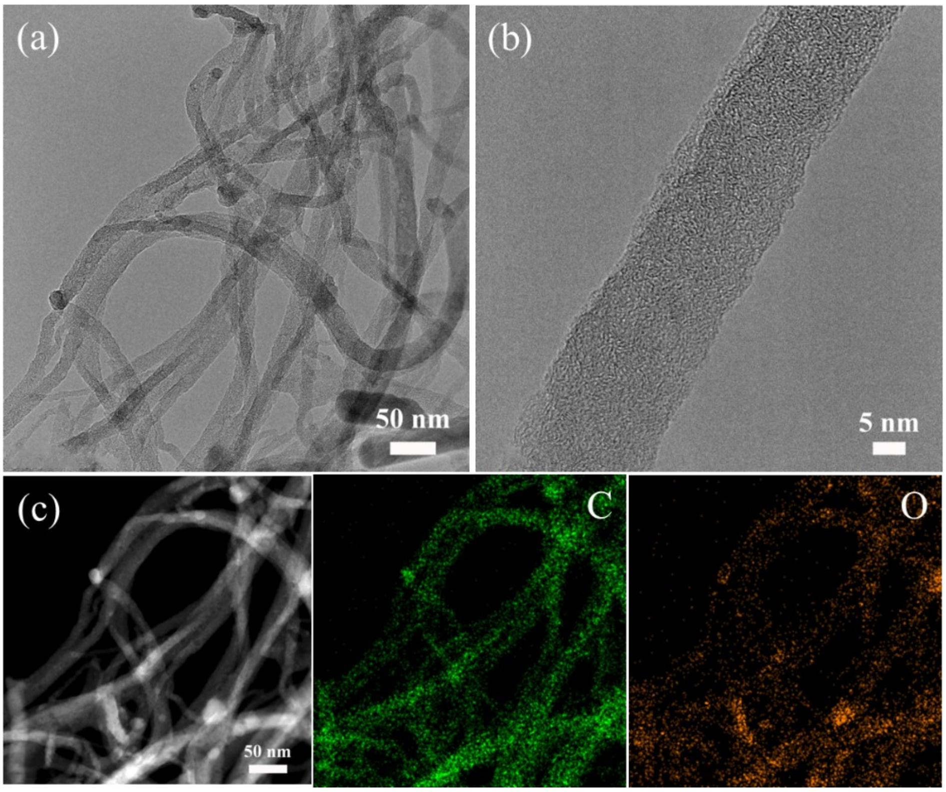

Fig. S3. (a) TEM image, (b)HRTEM, and (c) HAADF-STEM and the corresponding EDX elemental mapping images of CBC.

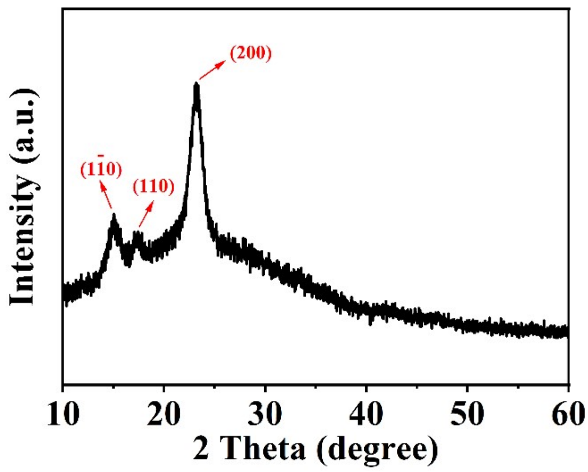

Fig. S4. XRD patterns of BC.

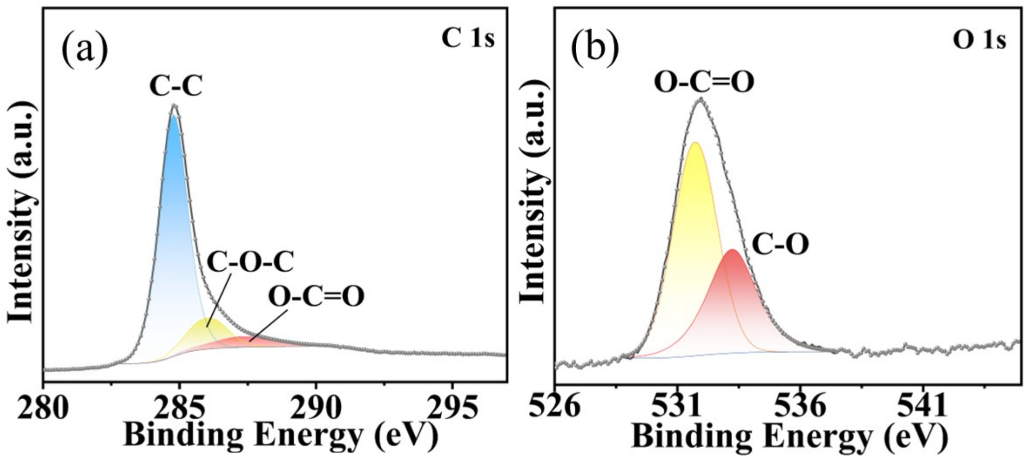

Fig. S5. high-resolution XPS spectra of (a) C 1s, and (b) O 1s of CBC.

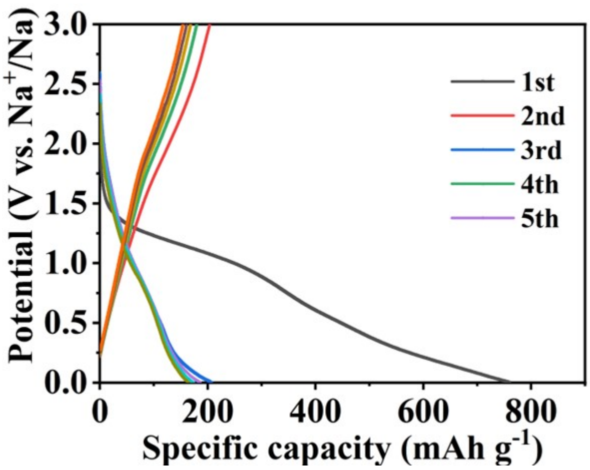

Fig. S6. GCD curves at 0.1 A g^{-1} of CBC.

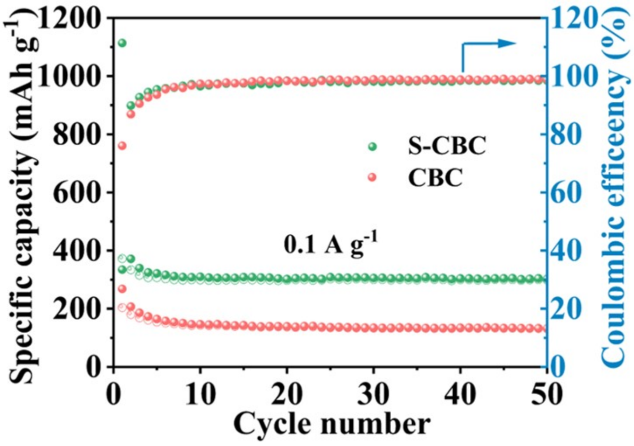

Fig. S7. Cyclic performance at 0.1 A g^{-1}.

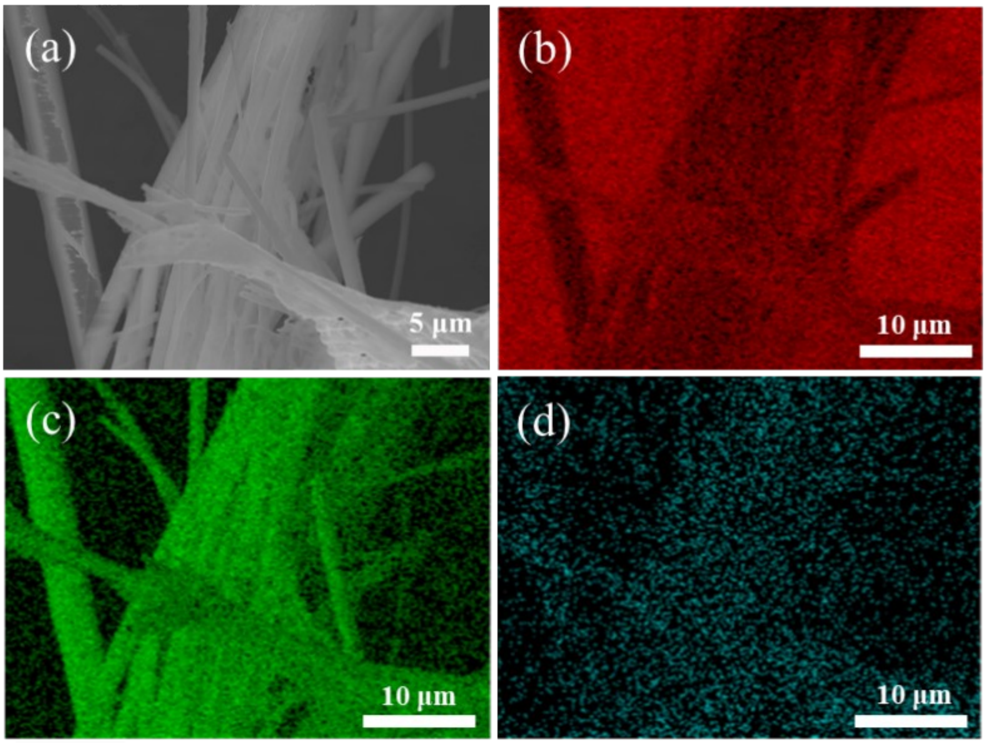

Fig. S8. The SEM image of S-CBC after 1000 cycles under 2 A g^{-1} .

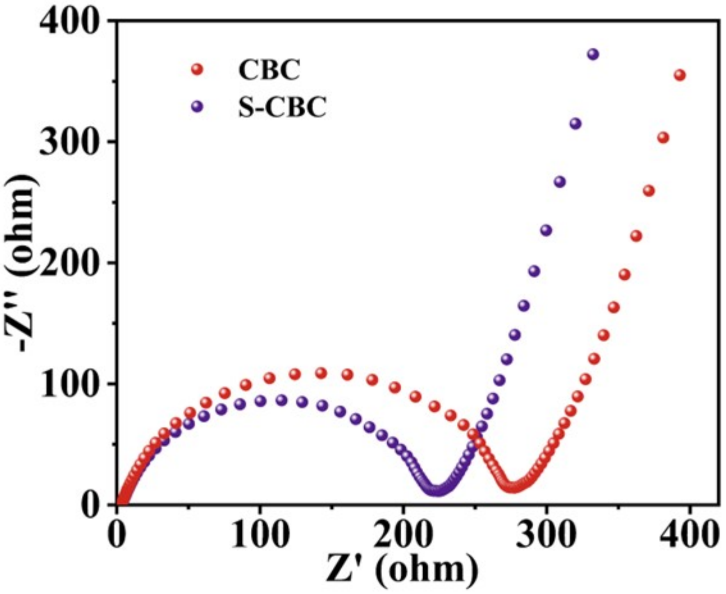

Fig. S9. EIS curves of S-CBC and CBC after 100 cycles under 0.1 A g^{-1} .

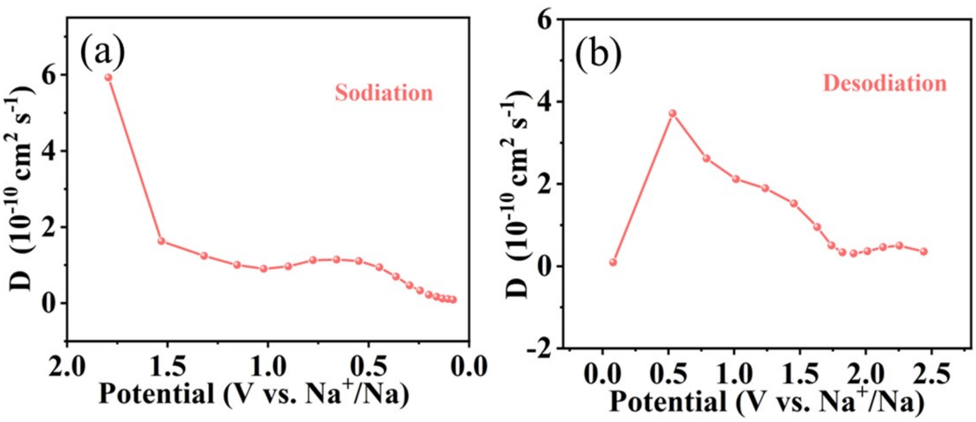

Fig. S10. The (a) Sodiation process and (b) Desodiation process of S-CBC.

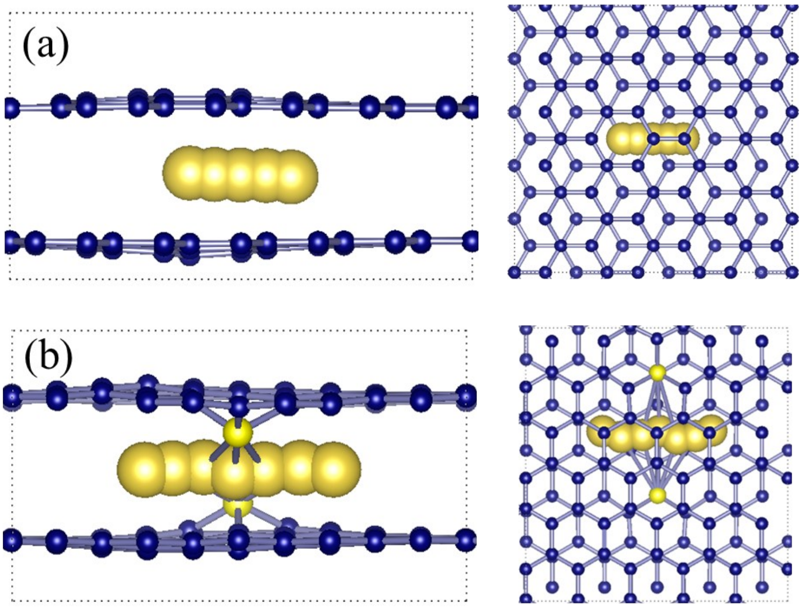

Fig. S11. The Na migration model of (a) pure carbon material and (b)S-doped carbon material.

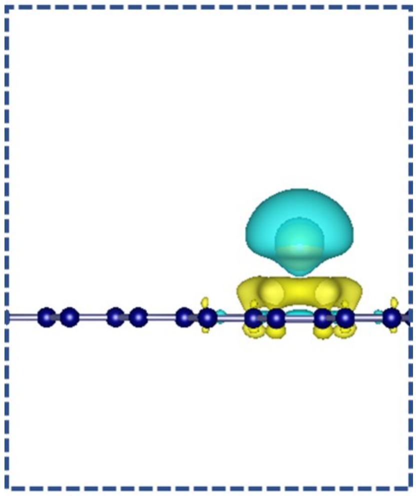

Fig. S12. The corresponding side view of electron density difference over CBC.

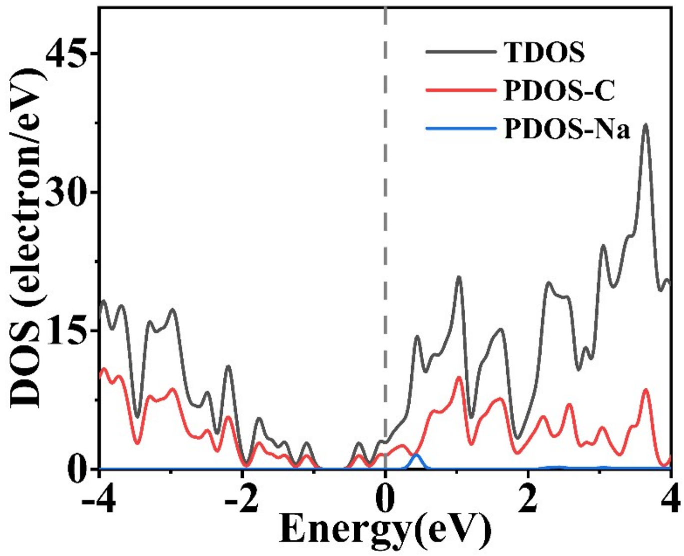

Fig. S13. The density of states of pure carbon.

Table S1. Comparison of electrochemical performances of our work and some other carbon anodes for Na-ion batteries.

Anode	Electrolyte	Voltage range V	Current density A g^{-1}	Specific capacity mAh g^{-1}	Cycle number	Refere-nce
HHPC-1100	1.0 mol L^{-1} $NaClO_4$ in EC / DEC	0.01–2.5	1	126.3	1000	1
KHC-1300	1.0 mol L^{-1} $NaClO_4$ in EC / DEC	0.01-2	0.2 1	205 96	300	2
SNC	1.0 mol L^{-1} $NaClO_4$ in PC	0.01-3	0.1 1	200 100	100 1000	3
F-CNTs	1.0 mol L^{-1} $NaClO_4$ in EC/PC	0.01-3	1 0.1	145 193	 200	4

N-CNTs	1.0 mol L^{-1} $NaPF_6$ in DME and EC/DMC	0.0- 2.5	0.05 0.5	290.3 147.1	 1000	5
TiO_2/CFC	1.0 mol L^{-1} $NaPF_6$ in EC/DMC/EMC and FEC	1.2-4.3	1	148.7	2000	6
HCP	1.0 mol L^{-1} $NaClO_4$ in EC / PC and FEC	0.01-2	2 0.2	176.8 286.5	1000 1000	7
NTO/CT	1.0 mol L^{-1} $NaClO_4$ in EC / DEC	0.01–2.5	1	130	1000	8
CNF@NPC	1.0 mol L^{-1} $NaClO_4$ in EC / DEC	0.01-3	0.1 0.5	240 148.8	100 400	9
PGFs	1.0 mol L^{-1} $NaClO_4$ in EC / DMC	0.01-3	0.05 1	195 111	50 1000	10
SN-HCSs	1.0 mol L^{-1} $NaClO_4$ in EC / DEC with FEC	0.01-3	0.5	169	2000	11
N/S-CS	1.0 mol L^{-1} $NaClO_4$ in EC / PC	0.01-3	1	155	2000	12
GPC	1.0 mol L^{-1} $NaClO_4$ in EC / DEC	0.01-3	0.5 0.05	145.6 284.8	600 60	13
PNCNs	1.0 mol L^{-1} $NaClO_4$ in PC / FEC	0.01-3	1 0.1	158 246.5	1000 100	14
N-CNFs	1.0 mol L^{-1} $NaClO_4$ in EC / DMC	0.001-2.5	1	150	200	15
SG	1.0 mol L^{-1} $NaPF_6$ in EC/DEC	0.001-3	1 2	150 133	200 100	16
S-CNF	1.0 mol L^{-1} $NaClO_4$ in EC / PC and FEC	0.01-3	0.1 2	302.9 177.6	50 1000	This work

HHPC: multi-heteroatom self-doped hierarchical porous carbon; KHC: kelp-derived hard carbon; SNC: sulfur-doped nitrogen-rich carbon nanosheets; F-CNTs: flame-synthesized carbon nanotubes; N-CNTs: N-doped carbon nanotubes; TiO_2/CFC: TiO_2 nanorods/carbon fiber cloth; HCP: hard carbon paper; GF//NTO/CT: 3D flexible $Na_2Ti_3O_7$ nanosheet arrays/carbon textile; CNF@NPC: carbon nanofiber@nitrogen-doped porous carbon; PGFs: Porous graphene films; SN-HCSs: SN-co-doped hollow carbon spheres; N/S-CS: N/S-co-doped porous carbon sheets; GPC: Graphene-based phosphorus-doped carbon; PNCNs: Phosphorus doped nitrogen-rich carbon nanosheets; N-CNFs: Nitrogen-doped carbon nanofibers; SG: sulfur-doped graphene.

Reference：

[1] C. Chen, Y. Huang, Z. Meng, Z. Xu, P. Liu, T. Li, Multi-heteroatom doped porous carbon derived from insect feces for capacitance-enhanced sodium-ion storage, Journal of Energy Chemistry, 54 (2021) 482-492.

[2] P. Wang, X. Zhu, Q. Wang, X. Xu, X. Zhou, J. Bao, Kelp-derived hard carbons as advanced anode materials for sodium-ion batteries, Journal of Materials Chemistry A, 5 (2017) 5761-5769.

[3] L. Bai, Y. Sun, L. Tang, X. Zhang, J. Guo, Sulfur and nitrogen co-doped carbon nanosheets for improved sodium ion storage, Journal of Alloys and Compounds, 868 (2021).

[4] W. Han, Y. Zhou, T. Zhu, H. Chu, Combustion synthesis of defect-rich carbon nanotubes as anodes for sodium-ion batteries, Applied Surface Science, 520 (2020).

[5] Y. Zhao, Z. Hu, C. Fan, Z. Liu, R. Zhang, S. Han, J. Liu, J. Liu, Constructing high-performance N-doped carbon nanotubes anode by tuning interlayer spacing and the compatibility mechanism with ether electrolyte for sodium-ion batteries, Chemical Engineering Journal, 446 (2022).

[6] S. Liu, Z. Luo, G. Tian, M. Zhu, Z. Cai, A. Pan, S. Liang, TiO_2 nanorods

grown on carbon fiber cloth as binder-free electrode for sodium-ion batteries and flexible sodium-ion capacitors, Journal of Power Sources, 363 (2017) 284-290.

[7] B.H. Hou, Y.Y. Wang, Q.L. Ning, W.H. Li, X.T. Xi, X. Yang, H.J. Liang, X. Feng, X.L. Wu, Self-Supporting, Flexible, Additive-Free, and Scalable Hard Carbon Paper Self-Interwoven by 1D Microbelts: Superb Room/Low-Temperature Sodium Storage and Working Mechanism, Adv Mater, 31 (2019) e1903125.

[8] S. Dong, L. Shen, H. Li, G. Pang, H. Dou, X. Zhang, Flexible Sodium-Ion Pseudocapacitors Based on 3D $Na_2Ti_3O_7$Nanosheet Arrays/Carbon Textiles Anodes, Advanced Functional Materials, 26 (2016) 3703-3710.

[9] Z. Zhang, J. Zhang, X. Zhao, F. Yang, Core-sheath structured porous carbon nanofiber composite anode material derived from bacterial cellulose/polypyrrole as an anode for sodium-ion batteries, Carbon, 95 (2015) 552-559.

[10] X. Zhang, J. Zhou, C. Liu, X. Chen, H. Song, A universal strategy to prepare porous graphene films: binder-free anodes for high-rate lithium-ion and sodium-ion batteries, Journal of Materials Chemistry A, 4 (2016) 8837-8843.

[11] J. Ye, J. Zang, Z. Tian, M. Zheng, Q. Dong, Sulfur and nitrogen co-doped hollow carbon spheres for sodium-ion batteries with superior cyclic and rate performance, Journal of Materials Chemistry A, 4 (2016) 13223-

13227.
[12] L. Wang, L. Hu, W. Yang, D. Liang, L. Liu, S. Liang, C. Yang, Z. Fang, Q. Dong, C. Deng, N/S-Co-Doped Porous Carbon Sheets Derived from Bagasse as High-Performance Anode Materials for Sodium-Ion Batteries, Nanomaterials (Basel), 9 (2019).
[13] G. Ma, Z. Xiang, K. Huang, Z. Ju, Q. Zhuang, Y. Cui, Graphene-Based Phosphorus-Doped Carbon as Anode Material for High-Performance Sodium-Ion Batteries, Particle & Particle Systems Characterization, 34 (2017).
[14] Y. Zhang, L. Li, W. Hong, T. Qiu, L. Xu, G. Zou, H. Hou, X. Ji, S. Li, Influence of P doping on Na and K storage properties of N-rich carbon nanosheets, Materials Chemistry and Physics, 236 (2019).
[15] J. Zhu, C. Chen, Y. Lu, Y. Ge, H. Jiang, K. Fu, X. Zhang, Nitrogen-doped carbon nanofibers derived from polyacrylonitrile for use as anode material in sodium-ion batteries, Carbon, 94 (2015) 189-195.
[16] X. Wang, G. Li, F.M. Hassan, J. Li, X. Fan, R. Batmaz, X. Xiao, Z. Chen, Sulfur covalently bonded graphene with large capacity and high rate for high-performance sodium-ion batteries anodes, Nano Energy, 15 (2015) 746-754.